THE JOURNAL OF PHYSICAL CHEMISTRY B

Article

Cite This: J. Phys. Chem. B XXXX, XXX, XXX−XXX

pubs.acs.org/JPCB

Effects of Trimethylamine-*N*-oxide (TMAO) on Hydrophobic and Charged Interactions

Zhaoqian Su, Gopal Ravindhran, and Cristiano L. Dias*

Department of Physics, New Jersey Institute of Technology, University Heights Newark, New Jersey 07102-1982, United States

Supporting Information

ABSTRACT: Effects of trimethylamine-*N*-oxide (TMAO) on hydrophobic and charge−charge interactions are investigated using molecular dynamics simulations. Recently, these interactions in model peptides and in the Trp-Cage miniprotein have been reported to be strongly affected by TMAO. Neopentane dimers and Na^+Cl^- are used, here, as models for hydrophobic and charge−charge interactions, respectively. Distance-dependent interactions, i.e., potential of mean force, are computed using an umbrella sampling protocol at different temperatures which allows us to determine enthalpy and entropic energies. We find that the large favorable entropic energy and the unfavorable enthalpy, which are characteristic of hydrophobic interactions, become smaller when TMAO is added to water. These changes account for a negligible effect and a stabilizing effect on the strength of hydrophobic interactions for simulations performed with Kast and Netz models of TMAO, respectively. Effects of TMAO on the enthalpy are mainly due to changes in terms of the potential energy involving solvent−solvent molecules. At the molecular level, TMAO is incorporated in the solvation shell of neopentane which may explain its effect on the enthalpy and entropic energy. Charge−charge interactions become stronger when TMAO is added to water because this osmolyte decreases the enthalpic penalty of bringing Na^+ and Cl^- close together mainly by affecting ion−solvent interactions. TMAO is attracted to Na^+, becoming part of its solvation shell, whereas it is excluded from the vicinity of Cl^-. These results are more pronounced for simulation performed with the Netz model which is more hydrophobic and has a larger dipole moment compared to the Kast model of TMAO.

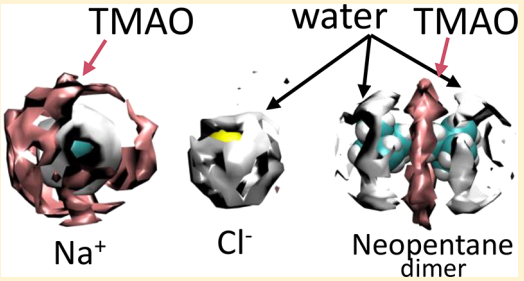

INTRODUCTION

Organic osmolytes are small solutes used by various organisms to regulate the water content of their cells.[1,2] Accordingly, they form part of the aqueous environments in which biochemical reactions in living systems take place affecting the stability of different molecular structures. This has led to their classification into protecting or denaturant osmolytes.[2−4] Denaturant osmolytes comprise the class of organic molecules that favor unfolded conformations over the native state of proteins. Urea and guanidine are among the most studied denaturants.[5] The former is found at high concentrations in mammalian kidneys, and it is a major osmolyte in marine elasmobranch fishes. The denaturant effect of urea can be rationalized by its favorable interactions with the protein surface. This favors the unfolded state which is characterized by protein conformations with larger solvent exposed surface area.[6−11] Conversely to denaturants, the presence of protecting osmolytes in solution favors the native state of proteins.[12] Trimethylamine *N*-oxide (TMAO) is an example of a protecting osmolyte that counteracts effects of water stresses allowing organisms to endure extreme conditions.[1] For instance, deep-sea creatures prevent water stresses by elevating TMAO levels in their body.[13,14] A molecular understanding of the effects of TMAO on proteins is still under debate despite intensive studies.[15]

The exclusion of TMAO from the vicinity of the protein provides an explanation for its stabilizing effect.[16−18] Favorable TMAO−water interactions contribute to this exclusion[19−25] which may be more pronounced close to the backbone of the protein.[25−29] Accordingly, polyglycine, which is a model of protein backbone, was reported to adopt more compact conformations in aqueous TMAO solutions than in pure water.[30,31] However, TMAO has also been shown to stabilize some nonpolar polymers through direct interactions.[32,33] This challenges the view that TMAO exclusion from the protein surface is its only/main mechanism of action. TMAO may also act as a crowding agent,[34,35] or/and it may weaken hydrogen bonds between the protein and water molecules.[35] A recent study showed that TMAO can interact favorably with the residues of the protein that are exposed to the solvent in the unfolded state.[36] In this study, TMAO was not excluded from air−water or polypeptide−water interfaces which is a result supported by both experiments and computer simulations.[23,37] Recently, the presence of TMAO around nonpolar side chains was found to correlate with the swelling of nonpolar peptides as well as with the destabilization of the hydrophobic core in the Trp-cage miniprotein.[31] In this computational study, TMAO was shown to strengthen charge−charge interactions which

Special Issue: Ken A. Dill Festschrift

Received: November 30, 2017
Revised: February 17, 2018
Published: February 26, 2018

DOI: 10.1021/acs.jpcb.7b11847
J. Phys. Chem. B XXXX, XXX, XXX−XXX

favored compact conformations of peptides flanked with oppositely charged termini and increased the stability of the native state of Trp-cage.[31] Thus, TMAO may have opposing effects on hydrophobic and charge−charge interactions which may be key to understanding its stabilizing mechanism on proteins. Here, we use simple compounds to provide further insights into these effects of TMAO.

Previous studies have shown that TMAO has little effect on the strength of hydrophobic interactions between small hydrophobic compounds, e.g., methane (CH_4),[38−40] whereas this osmolyte has a nonzero effect on larger nonpolar molecules, e.g., neopentane (C_4H_{12}).[32,41] Effects on the latter depend on the force-field used to simulate TMAO. In particular, studies using a five-site model for neopentane (see Figure 1) reported that the penalty for transferring this

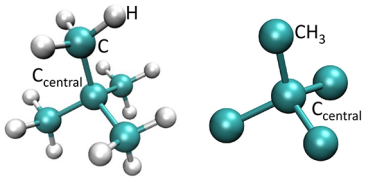

Figure 1. Molecular structures of the neopentane models used in this work.

nonpolar molecule to water was reduced and increased when simulations were performed using Kast and Netz force-fields for TMAO, respectively.[41] This implies that hydrophobic interactions can be made stronger or weaker with the addition of TMAO to the solution depending on simulation parameters. Effects of Kast TMAO on the interaction between a pair of neopentane molecules modeled as Lennard-Jones spheres have also been studied showing that this osmolyte weakens hydrophobic interactions.[42] Recently, the Kast model was shown to reproduce experimental properties of binary water−TMAO solutions.[43] However, the Netz model may provide a more realistic description of proteins in water−TMAO solutions as it was calibrated to reproduce experimental transfer free-energies of polyglycine from pure water to TMAO solutions.[44]

To study the effects of TMAO on distance-dependent interactions, i.e., potential of mean force (PMF), between hydrophobic molecules, we use a five-site and an all-atom representation of neopentane as well as Kast and Netz models to mimic TMAO. We use two representations of neopentane because effects of other organic molecules on hydrophobic interactions were reported to depend on the level of coarse-graining of the system.[45] In this paper, we also determine effects of TMAO on the distance-dependent enthalpy and entropy components associated with hydrophobic interactions. Extensive simulations are required to compute in these components of the free-energy, and therefore, they remain mostly unexplored. We find that both the large favorable entropy component and the unfavorable enthalpy, which are characteristic of hydrophobic interactions, become smaller when TMAO is added to water. These changes account for a negligible effect and a stabilizing effect on the association of nonpolar molecules when simulations are performed with Kast and Netz TMAO molecules in the all-atom model for neopentane. Effects of TMAO on the enthalpy are mainly due to changes in terms of the potential energy involving solvent−solvent molecules. We show that TMAO is incorporated in the solvation shell of neopentane, and we discuss how this may explain its effect on the enthalpy and entropy components. In this paper, we also study effects of TMAO on distance-dependent interactions between Na^+ and Cl^- ions. We find that charge−charge interactions become stronger when TMAO is added to water because this osmolyte reduces the enthalpic penalty of bringing Na^+ and Cl^- close together mainly by affecting ion−solvent interactions. At the molecular level, we find that TMAO is attracted to Na^+ becoming part of its solvation shell whereas it is excluded from the vicinity of Cl^-. These results for hydrophobic and charged interactions are more pronounced in the simulation performed using the Netz model which has a larger dipole moment and nonpolar moieties when compared to those of the Kast model.

METHODS

To investigate the effects of TMAO on hydrophobic and ionic interactions, we perform molecular dynamics simulations in the NPT ensemble at 1 atm and at four temperatures (273 K, 298, 338, and 368 K). The open-source Gromacs suite version 4.6.5 is used to perform these simulations.[46] The temperature is controlled using the v-rescale thermostat (τ_T = 1 ps), and pressure is fixed using the Parrinello−Rahman barostat (τ_P = 1 ps). A cutoff of 1.3 nm is used to account for short-range nonbonded interactions. Long-range electrostatics were calculated using the Particle Mesh Ewald (PME) algorithm with a grid spacing of 0.13 nm and a 1.3 nm real-space cutoff.

Simulations are conducted using the TIP3P water model, the Kast[47] and Netz[44] models for TMAO, the five-site OPLS,[48] the all-atom AMBER models for neopentane (see Figure 1 and Table 1), and the AMBER model for Na^+ and Cl^-.[49]

Table 1. Lennard-Jones Parameters and Partial Charges of Neopentane Models Used in This Work

force-field	atom	σ (nm)	ϵ (kJ/mol)	charge (e)
all-atom model	$C_{central}$	0.339967	0.45773	0.544
	C	0.339967	0.45773	−0.298
	H	0.264953	0.06569	0.054
united model	$C_{central}$	0.38000	0.20920	0
	CH_3	0.39600	0.60668	0

Parameters of TMAO force-fields including combination rules are given as Supporting Information. Notice that the Netz model has been parametrized in solutions containing SPC/E water whereas it is used combined with TIP3P water in this study which is the recommended water model for the AMBER force-field. Effects of Netz TMAO on the five-site model of neopentane embedded in TIP3P (Figure 2 in this study) and in SPC/E water (reported in ref 41) are in qualitative agreement. Moreover, TMAO has been shown to have the same qualitative effect on the conformation of peptides (poly leucine and $A\beta_{16-22}$) that are embedded in TIP3P or SPC/E water.[31] This suggests that the Netz model is robust, at least qualitatively, against details of the water model. Notice that a new version of the Kast model has recently been developed to account for the density of aqueous TMAO solutions at high pressures.[50] This new Kast model has not been considered in this study.

To compute the free-energy landscape describing neopentane−neopentane and Na^+−Cl^- interactions, we use an umbrella sampling protocol. For the reaction coordinate of these interactions, we use the distance ξ between central atoms

DOI: 10.1021/acs.jpcb.7b11847
J. Phys. Chem. B XXXX, XXX, XXX−XXX

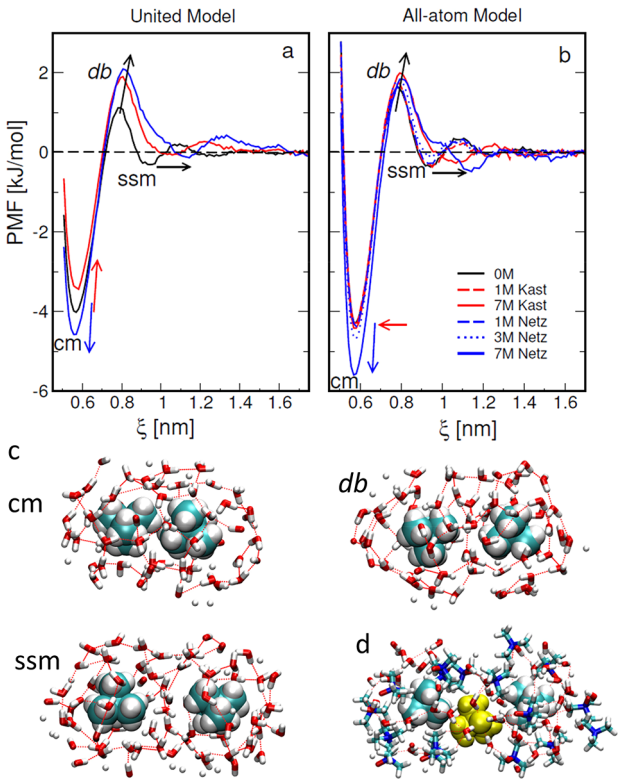

Figure 2. Potential of mean force (PMF) of a neopentane dimer in pure water (black) and aqueous TMAO solutions (red and blue) computed using (a) the five-site united model and (b) the all-atom model of neopentane. PMF values computed at ξ = 1.7 nm are used as our reference, i.e., zero value. (c) Characteristic configurations of neopentane dimers at cm, *db*, and ssm in pure water. Water molecules within a distance of 0.65 nm from $C_{central}$ are also shown. Neopentane and water molecules are depicted using van der Waals and licorice representations, respectively. Dotted red lines correspond to hydrogen bonds. (d) Characteristic ssm configuration at 7 M Kast TMAO solution. A TMAO molecule in between the neopentane dimer is highlighted in yellow.

of neopentane molecules in the range 0.5−1.75 nm, and the distance between ions in the range 0.2−1.1 nm. In the different windows of the umbrella sampling protocol, neopentanes and ions are restrained to their equilibrium distance by a spring. The equilibrium distances of springs in neighboring windows differ in steps of 0.05 nm, and their spring constant is 4000 kJ mol^{-1} nm^{-2}. Each window is simulated for 150 ns, and the potential of mean force (PMF) is computed using the weighted histogram analysis method (WHAM).[51] Notice that the PMF increases with $-k_bT \log(\xi^2)$ due to the three-dimensional nature of ξ, where $-k_bT$ is the thermal energy. We subtract this dependence of the PMF on ξ, and the PMF at the last umbrella sampling window (ξ = 1.75 nm for neopentane dimers or ξ = 1.1 for Na^+−Cl^-) is shifted to zero. PMFs are computed from simulations in pure water (0 M), and at 3 and 7 M TMAO concentrations. See Supporting Information for a list of all simulations performed in this work.

The enthalpy and entropy components as a function of ξ are computed from the temperature dependence of the PMF. For each ξ distance, the temperature dependence of the PMF is fitted to the thermodynamic relation[52−54]

$$\mathrm{PMF}(\xi, T) = \Delta H_0(\xi) - T\Delta S_0(\xi) + \Delta C_{op}(\xi)\left[(T - T_0) - T\log\left(\frac{T}{T_0}\right)\right] \quad (1)$$

where $\Delta S_0(\xi)$, $\Delta H_0(\xi)$, and $\Delta C_{op}(\xi)$ correspond to changes in entropy, enthalpy, and heat capacity, respectively, at the reference temperature T_0 = 298 K. Notice that, with increasing temperature, the different states of the system shift to larger ξ-distances due to thermal expansion. For the range of temperatures in our simulations, this effect is negligible for charge−charge interactions, but it is significant for neopentane dimers (see Figure S1 in Supporting Information). To account for this effect, enthalpy and entropy components for neopentane are computed as a function of ξ/ξ_0, where ξ_0 is the reaction coordinate at the first minimum of the PMF.

RESULTS AND DISCUSSION

Effects of TMAO on Hydrophobic Interactions. *Potential of Mean Force.* Figure 2a,b shows the potential of mean force (PMF) of neopentane dimers in pure water (black) and in aqueous TMAO solutions (blue and red) at 298 K and 1 atm. These PMFs exhibit three distinct states which are the contact minimum (cm), the desolvation barrier (*db*), and the solvent-separated minimum (ssm).[55−59] At cm, the two neopentane molecules are in direct contact at a distance between their central carbon atoms of ξ = 0.58 nm. ssm occurs at a neopentane distance of ξ = 0.94 nm which is large enough to allow water molecules to occupy the space between the dimer. *db* occurs at ξ = 0.79 nm wherein water molecules cannot fit within the space between neopentanes. Configurations at *db* are, therefore, characterized by the presence of cavities between neopentane molecules. In Figure 2c, we depict characteristic conformations of these states for simulations performed in pure water for the all-atom neopentane model.

Stabilities of cm, *db*, and ssm depend on temperature, the concentration of TMAO, and the different force-fields used in the simulation. In Figure 2a, we study effects of TMAO on the PMF of the five-site model of neopentane. The addition of TMAO to water accounts for an increase and a decrease in the stability of cm when simulations are performed with Netz and Kast models, respectively; see blue and red arrows in Figure 2a. These results are consistent with the reported increase and decrease in transfer free-energies of neopentane from pure water to aqueous TMAO solutions for simulations performed with Netz and Kast models, respectively.[41] Notice that the geometric rule for cross-interactions of Lennard-Jones parameters is used to study the five-site model of neopentane in our study and in ref 41. In contrast to these force-field-dependent effects at cm, both Netz and Kast models account for an increase in the desolvation barrier and a shift in the position of ssm to larger distances. The later effect suggests that TMAO molecules, which are larger than water, occupy the space between neopentanes at ssm. A characteristic configuration illustrating the presence of TMAO in between neopentane molecules at ssm is shown in Figure 2d.

In Figure 2b, effects of TMAO on the PMF of the all-atom model of neopentane are shown. Similarly to its effect on the five-site model of neopentane, Netz TMAO increases the stability of cm, and it enhances the magnitude of the desolvation barrier whereas the position of ssm is shifted to larger distances. These effects are enhanced when the

DOI: 10.1021/acs.jpcb.7b11847
J. Phys. Chem. B XXXX, XXX, XXX−XXX

concentration of TMAO is increased from 1 to 7 M. Kast TMAO molecules also increase the magnitude of the desolvation barrier, and they shift ssm to larger distances. However, conversely to their destabilizing effect on cm in the five-site model of neopentane, Kast TMAO molecules have no significant effect on the stability of cm for the all-atom neopentane model at concentrations of both 1 and 7 M. These results show that simulations performed with the Kast model are more strongly dependent on the details of the nonpolar compound model than simulations performed with the Netz model.

Enthalpy and Entropy Component. To provide insights into how Kast and Netz models of TMAO affect the interaction between neopentane molecules, we show in Figure 3 the

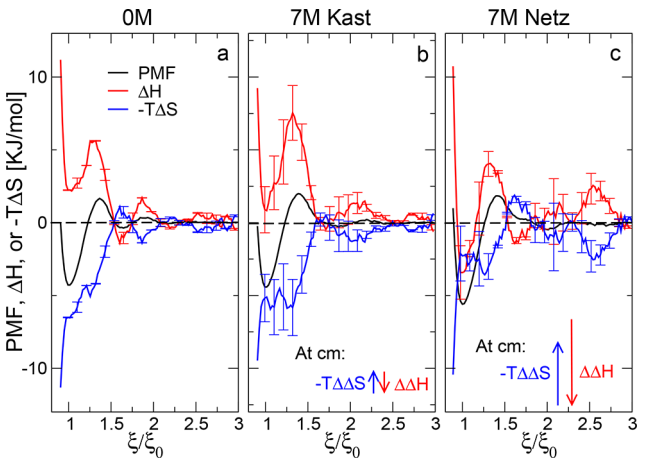

Figure 3. Decomposition of the PMF (black) into enthalpy (red) and entropy (blue) components at T_0 in (a) pure water and (b, c) aqueous TMAO solutions as a function of ξ/ξ_0. See Methods section. Effects of TMAO on the enthalpy (red) and entropy (blue) components at cm are shown by arrows. Error bars are estimated from curve fitting.

decomposition of the PMF into enthalpy (ΔH) and entropy ($-T\Delta S$) components, i.e., $\mathrm{PMF}(\xi) = \Delta H(\xi) - T\Delta S(\xi)$. This decomposition is performed for the all-atom model of neopentane in pure water and in aqueous solutions containing 7 M Kast or 7 M Netz TMAO molecules. These high TMAO concentrations were chosen for further analysis as they beget discernible effects in the PMF of neopentane dimers in Figure 2b. In pure water (panel a), the interaction between neopentane molecules, i.e., small ξ distances, is disfavored by enthalpy ($\Delta H_{\mathrm{water}} > 0$) whereas it is favored by entropy ($-T\Delta S_{\mathrm{water}} < 0$).[54,60,61] This decomposition can be rationalized by considering that water molecules around nonpolar solutes, i.e., shell water, have a lower entropy and a lower enthalpy than bulk water.[60,62] During the formation of cm, some shell water molecules are transferred to the bulk accounting for the increase in entropy (or decrease in $-T\Delta S_{\mathrm{water}}$) and the increase in enthalpy of Figure 3a.

In Figure 3b,c, we show how the enthalpy (ΔH_{TMAO}) and the entropy ($-T\Delta S_{\mathrm{TMAO}}$) components change as a function of ξ in aqueous 7 M TMAO solutions. Arrows in these figures depict how ΔH_{TMAO} and $-T\Delta S_{\mathrm{TMAO}}$ at cm compare to $\Delta H_{\mathrm{water}}$ and $-T\Delta S_{\mathrm{water}}$, respectively. In other words, arrows show $\Delta\Delta H \equiv \Delta H_{\mathrm{TMAO}} - \Delta H_{\mathrm{water}}$ and $-T\Delta\Delta S \equiv -T\Delta S_{\mathrm{TMAO}} + T\Delta S_{\mathrm{water}}$. For both Netz and Kast models at cm, $-T\Delta\Delta S > 0$ which implies that the increased order of solvent molecules in the vicinity of neopentane (when compared to bulk water) is less important in TMAO solutions than in pure water. In contrast, for Netz and Kast models at cm, $\Delta\Delta H < 0$. To provide molecular insights into $\Delta\Delta H$, changes in the potential energy of the system when the dimer is brought to cm from noninteracting distances are decomposed into contributions from neopentane−neopentane ($\Delta E^{\mathrm{Neo-Neo}}$), neopentane−solvent ($\Delta E^{\mathrm{Neo-Sol}}$), and solvent−solvent ($\Delta E^{\mathrm{Sol-Sol}}$) interactions. Notice that the volume V of the system does not change significantly when dimers are brought to interact at cm[58] and $p\Delta V$ (where p is the pressure of the system) is found to be negligible. Figure 4 depicts how the

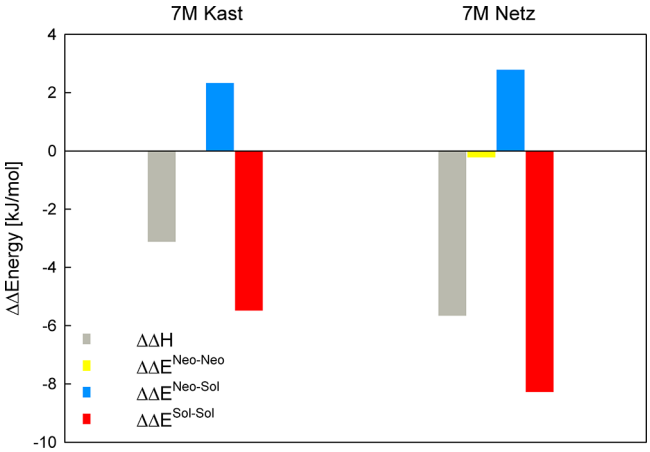

Figure 4. Changes in the enthalpy of cm formation, i.e., $\Delta\Delta H$ (in gray), due to the addition of Kast (left) and Netz (right) TMAO molecules to water for neopentane dimers. These changes are decomposed into contributions from neopentane−neopentane $\Delta\Delta E^{\mathrm{Neo-Neo}}$ (yellow), neopentane−solvent $\Delta\Delta E^{\mathrm{Neo-Sol}}$ (blue), and solvent−solvent $\Delta\Delta E^{\mathrm{Sol-Sol}}$ (red) interactions. Notice that the gray column corresponds to the $\Delta\Delta H$ computed at cm in Figure 3b,c. These results indicate that solvent−solvent interactions, i.e., $\Delta\Delta E^{\mathrm{Sol-Sol}}$, are the main energetic term accounting for the change in $\Delta\Delta H$ when TMAO is added to water.

different potential energy terms computed in TMAO solution compare with the respective terms in pure water simulation, i.e., $\Delta\Delta E = \Delta E_{7\mathrm{M}} - \Delta E_{0\mathrm{M}}$. This figure shows that the main term accounting for the negative $\Delta\Delta H$ is solvent−solvent interactions which suggests that bonding states of the solvent in the vicinity of neopentane are less favorable in aqueous TMAO solutions than in pure water. This implies that the transfer of solvent molecules from the first shell to the bulk during cm formation accounts for a smaller $\Delta E^{\mathrm{Sol-Sol}}$ in TMAO solution than in pure water. Notice that $\Delta\Delta E^{\mathrm{Neo-Sol}} > 0$ which implies that neopentane−solvent interactions become more favorable when TMAO is added to water. This term for charge−charge interactions behaves very differently as will be shown in Figure 8.

In summary, both the enthalpic penalty and the favorable entropic contribution of the hydrophobic effect become less important when TMAO is added to water. Moreover, the solvent−solvent interaction in the shell provides the driving force for TMAO's enthalpic stabilization. These effects are more prominent for the Netz model.

Solvation Shell around Neopentane. To provide insights into effects of TMAO on the solvation of neopentane molecules, Figure 5 shows radial distribution functions (RDFs) of the central carbon of neopentane, i.e., $\mathrm{C_{central}}$, and different atoms of TMAO, i.e., oxygen ($\mathrm{O_{TMAO}}$ in red), nitrogen ($\mathrm{N_{TMAO}}$ in blue), or carbon ($\mathrm{C_{TMAO}}$ in black). The RDF of

DOI: 10.1021/acs.jpcb.7b11847
J. Phys. Chem. B XXXX, XXX, XXX−XXX

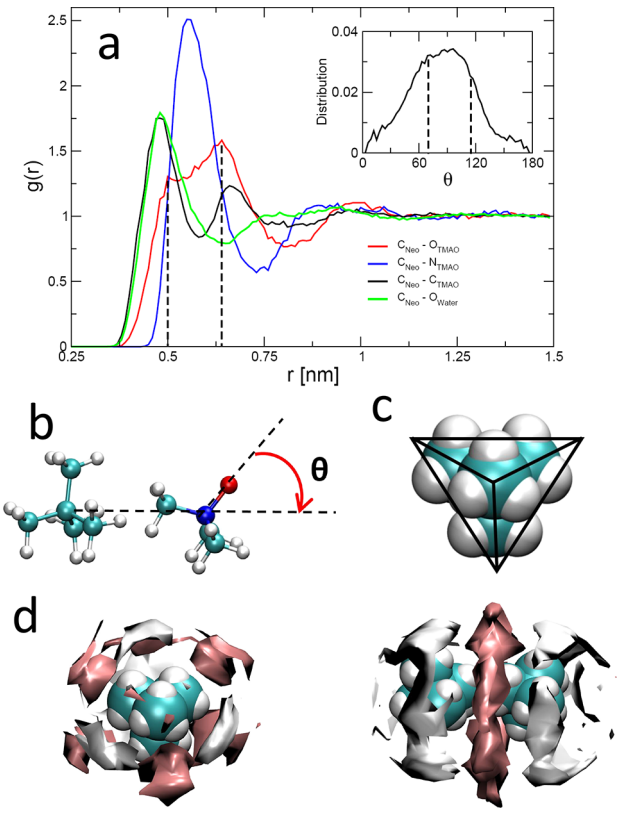

Figure 5. Solvation of the all-atom model of neopentane in 7 M Kast solution at 298 K. (a) Radial distribution functions of central carbon of neopentane and different groups of TMAO (oxygen in red, nitrogen in blue and carbon in black) or oxygen atom of water (in green). These functions are computed when neopentane molecules are far apart, i.e., at ξ = 1.70 nm. The inset of panel a shows the distribution of θ for TMAO molecules in the solvation shell. (b) Snapshot of a TMAO molecule within the solvation shell of neopentane showing its angle θ. (c) Tetrahedral (in black) formed by methyl groups of neopentane. (d) Spatial distribution functions of TMAO (pink color) and water (silver color) around neopentane in 7 M Kast TMAO solutions at ξ = 1.7 nm (left) and at ξ = 0.58 nm (right). Isovalues for TMAO and water are 8 and 9.

$C_{central}$ and oxygen atoms of water (O_{water} in green) is also shown. These RDFs are computed in 7 M Kast TMAO simulations when neopentane molecules are far apart from each other, i.e., ξ = 1.7 nm. As part of the Supporting Information (SI), we show that the position of the different peaks of the RDF does not change significantly when simulations are performed in 1 M Kast TMAO solution or when the neopentane pair is at cm, i.e., at ξ = 0.58 nm.

The solvation shell of neopentane defined by the first peak in the $C_{central}$–O_{water} RDF comprises 36 water molecules that are located at distances smaller than 0.65 nm from $C_{central}$. Several atoms of TMAO are located within this first solvation shell as shown by the first peak in their RDF in Figure 5a. Accordingly, by integrating the first peak of the $C_{central}$–N_{TMAO} RDF up to its first minimum, we find that 15.6 and 2.2 TMAO molecules are located within the first solvation shell when simulations are performed in 7 and 1 M Kast TMAO solutions, respectively.

The broad first peak in the $C_{central}$–O_{TMAO} RDF can be deconvoluted into two peaks: one located at 0.5 nm and the other at 0.64 nm. These peaks can be interpreted by studying the angle θ formed by the lines connecting N_{TMAO}–O_{TMAO} and $C_{central}$–N_{TMAO} pairs of atoms as shown in Figure 5b. Average angles of 114° and 69° are found to correspond to the peaks located at 0.5 and 0.64 nm. These angles are shown by dashed vertical lines in the inset of Figure 5a where the distribution of θ for all TMAO molecules in the first shell is also shown. This distribution is center at 87°, implying that the vector formed by N_{TMAO}–O_{TMAO} atoms is on average tangential to the surface of neopentane. This implies that some of the CH_3 groups of TMAO are completely solvated whereas others are interacting with neopentane. The two peaks in the $C_{central}$–C_{TMAO} RDF (black line) reflect these two states. The peak located at short distances, i.e., 0.48 nm, corresponds to CH_3 groups of TMAO that are in contact with neopentane whereas the peak at 0.66 nm corresponds to CH_3 groups that are solvated. These configurations of TMAO have been reported in experiments and computer simulations for large hydrophobic–water interfaces.[23,37] The insights brought up by studying RDF in Figure 5a suggest that water in the first solvation shell of neopentane is disturbed by the presence of TMAO. In pure water, this shell accounts for a large favorable change in the entropy component ($-T\Delta S < 0$) and an unfavorable change in enthalpy ($\Delta H > 0$) when small nonpolar molecules are brought close together, see Figure 3a. By perturbing the first solvation shell, TMAO reduces these entropic and enthalpic effects. This gives rise to interactions that are less entropic in nature (i.e., $-T\Delta\Delta S > 0$) with a smaller enthalpic penalty ($\Delta\Delta H < 0$), see Figure 3b,c. Notice that the overall result of these effects on the PMF is either negligible (due to an almost perfect enthalpy–entropy compensation) or increases the stability of the interaction between neopentane molecules for simulations performed with Kast or Netz models, respectively, see Figure 2b. This shows that enthalpy and entropy can be used to provide insights into the mechanism of action of TMAO even when this cosolvent does not account for significant changes in the free-energy of the system.

In Figure 5d, we show spatial distribution functions of TMAO (pink color) and water (silver color) around neopentane for simulations performed in 7 M Kast TMAO solution. Spatial distribution functions are computed by dividing the simulation box in bins of size 0.05 × 0.05 × 0.05 nm^3, and they are given as the ratio between the density of solvent molecules in the bin and the density of the solvent in an ideal fluid. In the left panel of Figure 5d, the two neopentane molecules are far apart from each other, i.e., ξ = 1.7 nm, and the spatial distribution is shown for only one of the neopentane molecules. For this state, TMAO is located preferentially along the edges of the tetrahedron formed by methyl groups of neopentane (see Figure 5c) whereas water is found preferentially in the center of the faces of this tetrahedron. Thus, we observe 6 TMAO clusters comprising 7.8 molecules and 4 water clusters comprising 18 molecules in the vicinity of a single neopentane. In the right panel of Figure 5d, the neopentane pair is at cm, i.e., ξ = 0.58 nm. For this state, TMAO accumulates in the middle ring of two neopentane molecules, and water is distributed laterally to the neopentane dimer.

Effects of TMAO on Charged Interactions. *Potential of Mean Force.* In Figure 6a, we show PMF describing the interaction between Na^+ and Cl^- ions in pure water (black) and aqueous TMAO solutions (red and blue). These PMFs are characterized by the presence of a contact minimum (cm), a desolvation barrier (*db*), a first-solvent-separated minimum (1st ssm), and a second-solvent-separated minimum (2nd ssm). Arrows in Figure 6a show the increased stability of cm states

DOI: 10.1021/acs.jpcb.7b11847
J. Phys. Chem. B XXXX, XXX, XXX–XXX

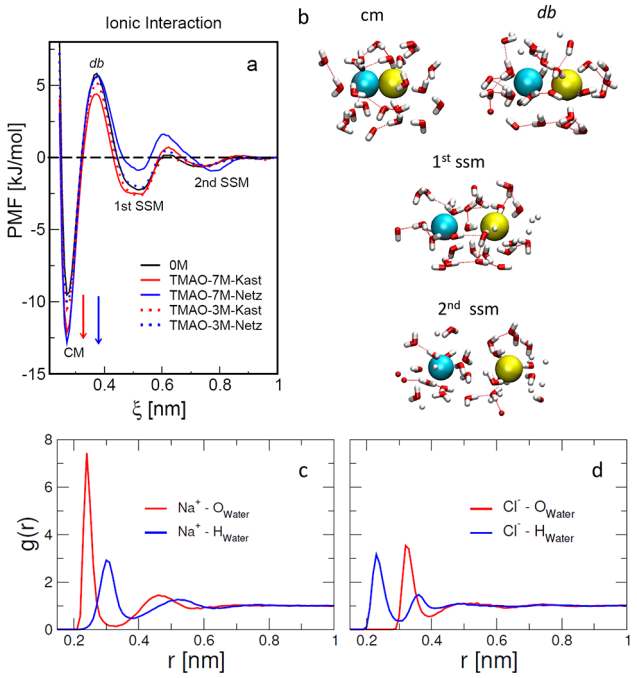

Figure 6. (a) Potential of mean force (PMF) for the interaction between Na^+ and Cl^- ions in pure water (black) and aqueous TMAO solutions (red and blue). PMF values computed at ξ = 1.1 nm are used as our reference, i.e., zero value. (b) Characteristic configurations of sodium (cyan) and chloride (yellow) at cm, *db*, 1st ssm, and 2nd ssm. Water molecules in the first solvation shell are shown in a licorice representation. Dotted lines correspond to hydrogen bonds. (c, d) RDFs of ion−O_{water} (red) and ion−H_{water} (blue) in pure water simulations when ions are far apart from each other, i.e., ξ = 1.1 nm.

when Kast or Netz TMAO molecules are added to water. *db* becomes smaller in simulations performed with Kast TMAO whereas the Netz model has little effect on the stability of this state. Surprisingly, we find that the Kast model stabilizes the first ssm while the Netz model destabilizes this state. In the Supporting Information (Figures S8 and S9), we provide an explanation for this behavior in terms of the distribution of TMAO and water at the first ssm. Notice that several force-fields, including the AMBER force-field used in this work, have been shown to reproduce the experimental transfer free-energy of sodium (−375 kJ/mol) and chloride (−347 kJ/mol) to pure water, which combined accounts for a free-energy change of 722 kJ/mol.[63] However, the distance-dependent interaction for Na^+ and Cl^- ions, i.e., position and magnitude of the PMF at different states, has been shown to depend on the force-field used in the simulation.[64] To estimate how effects of TMAO on charge−charge interactions are affected by the parametrization of Na^+ and Cl^-, we show in Figure S10 (Supporting Information) the PMF of NaCl computed using the Joung and Cheatham force-field.[65] These PMFs are computed in pure water and 7 M aqueous Kast solution. In these simulations, TMAO stabilizes both cm and first ssm while it reduces *db*. These trends are consistent with the ones shown in Figure 6.

In Figure 6b, we show characteristic configurations of the different states of the PMF. One and two layers of water molecules separate Na^+ and Cl^- ions in the first and second ssm, respectively. These ions are in contact, i.e., at close proximity, at cm whereas cavities in the space between them account for a large positive PMF at *db*. In Figure 6c,d, we show RDFs for ion−O_{water} and ion−H_{water} in simulations performed in 7 M Kast TMAO solution when ions are far apart from each other, i.e., ξ = 1.0 nm. From these RDFs, O_{water} peaks closer to Na^+ than H_{water} whereas the opposite order in first peaks is observed for Cl^-. This reflects the orientation of water molecules in the solvent first shell which is such that their hydrogen atoms, which have positive partial charges, point toward and away from Cl^- and Na^+ ions, respectively. These water configurations minimize the electrostatic energy between ions and the dipole moment of water. Notice that water structures around neopentane optimize the network of hydrogen bond in the solvation shell.

Enthalpy and Entropy. To provide insights into effects of TMAO on the distance-dependent interaction of Na^+ and Cl^- ions, we decompose the PMF into enthalpy (ΔH) and entropy ($-T\Delta S$) components in Figure 7. In pure water (panel a), the

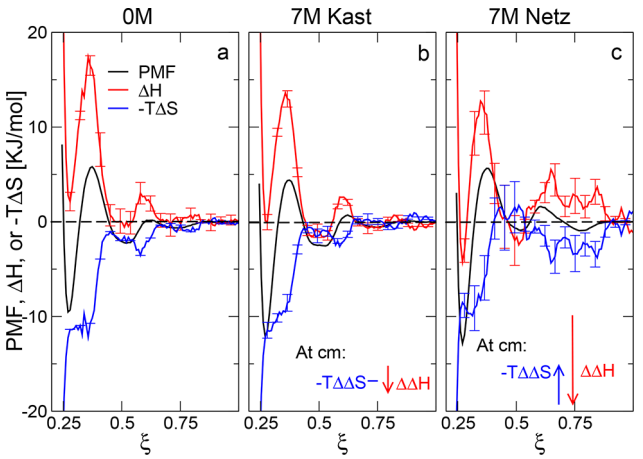

Figure 7. PMF of Na^+−Cl^- decomposed into enthalpy (red) and entropy (blue) components for simulations performed in (a) pure water, (b) 7 M Kast TMAO, and (c) 7 M Netz TMAO solutions at 298 K.

interaction between Na^+ and Cl^- ions is favored by entropy (blue), and it is opposed by enthalpy (red).[66] This reflects the reduced mobility of water in the first solvation shell around ions which emerges from strong electrostatic interactions between ions and the dipole moment of water molecules.[67] As Na^+ and Cl^- are brought close to each other, some waters in the first solvation shell are released into the bulk where they become more disordered accounting for a favorable change in the entropy component, see Figure 7a. Concurrently, the enthalpy of these released water molecules increases as they stop interacting with the ions.

The transfer of shell water to the bulk in the presence of TMAO reduces both the enthalpic penalty and the entropic gain associated with the formation of cm. This is represented by arrows in Figure 7b,c. In this figure, $\Delta\Delta H$ (red arrow) is larger than $-T\Delta\Delta S$ (blue arrow) at cm implying that enthalpy is not exactly compensated by entropy, and effects of TMAO are dominated by enthalpy. Other effects of TMAO are to reduce the enthalpic barrier and to increase the entropy component associated with the formation of cavities at *db*. Notice that effects of TMAO are more significant in the Netz model for which TMAO has a larger dipole moment associated with its nitrogen and oxygen atoms as well as a larger hydrophobicity related to CH_3 groups.

To provide molecular insights into the enthalpic stabilization of charge−charge interactions by TMAO at cm, i.e., $\Delta\Delta H < 0$,

DOI: 10.1021/acs.jpcb.7b11847
J. Phys. Chem. B XXXX, XXX, XXX−XXX

we decompose the potential energy of the system into contributions from ion−ion, ion−solvent, and solvent−solvent interactions. In Figure 8 we show how these potential energy terms computed in 7 M TMAO solution compare with the same terms computed in pure water; i.e., we show $\Delta\Delta E = \Delta E_{7M} - \Delta E_{0M}$. Figure 8 shows that the main term accounting for the negative $\Delta\Delta H$ comes from ion−solvent interactions. This suggests that solvent molecules bond less favorably with ions in TMAO solutions than in pure water. This implies that when solvent molecules in the first shell are transferred into the bulk during cm formation, $\Delta E^{Ion-Sol}$ increases less significantly in TMAO solutions than in pure water. This motivates the study of how TMAO is distributed in the vicinity of ions to weaken ion−solvent interactions in the next section.

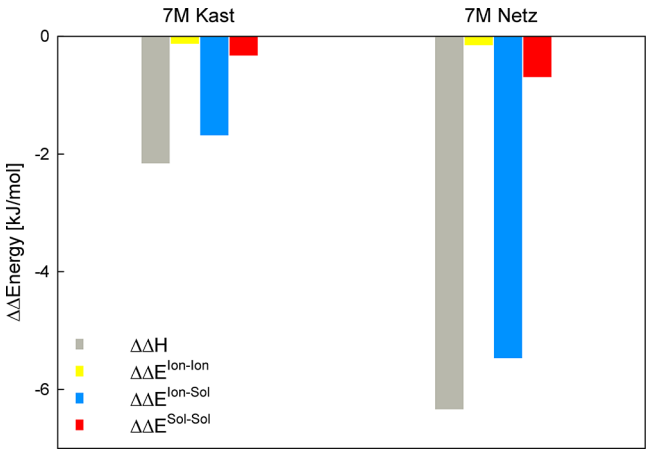

Figure 8. Changes in the enthalpy of cm formation, i.e., $\Delta\Delta H$ (in gray), due to the addition of Kast (left) and Netz (right) TMAO molecules to water for NaCl. These changes are decomposed into contributions from neopentane−neopentane $\Delta\Delta E^{Neo-Neo}$ (yellow), neopentane−solvent $\Delta\Delta E^{Neo-Sol}$ (blue), and solvent−solvent $\Delta\Delta E^{Sol-Sol}$ (red) interactions. Notice that the gray column correspond to the $\Delta\Delta H$ in Figure 7b,c. These results indicate that ion−solvent interactions, i.e., $\Delta\Delta E^{Ion-Sol}$, are the main energetic term accounting for the change in $\Delta\Delta H$ when TMAO is added to water.

Solvation Shell around Na^+ and Cl^- Ions. In Figure 9a,b, we show RDFs for the interaction between ions and O_{TMAO} (red line), N_{TMAO} (blue), or C_{TMAO} (black). RDFs describing the interactions between ions and O_{water} are also shown in green. These functions are computed in simulations performed at 7 M Kast TMAO solution when Na^+ and Cl^- ions are far apart from each other, i.e, at ξ = 1.1 nm. In Figure 9a, first peaks in the RDF of Na^+ and oxygen atoms of both water and TMAO occur at the same short distance of 0.24 nm. This attraction between Na^+ and oxygen accounts for a solvation shell containing 1.4 TMAO and 4.5 water molecules, respectively. In 3 M Kast TMAO solution (RDF not shown), the numbers of TMAO and water molecules in the solvation shell are 0.3 and 5.5, respectively. Notice that, in pure water (RDF not shown), the number of solvent molecules around Na^+ is 5.9. These numbers were obtained by integrating the first peaks in RDFs of Na^+−O_{TMAO} and Na^+−O_{water}. The lack of C_{TMAO} atoms in the first solvation shell of Na^+ (see Figure 9a)

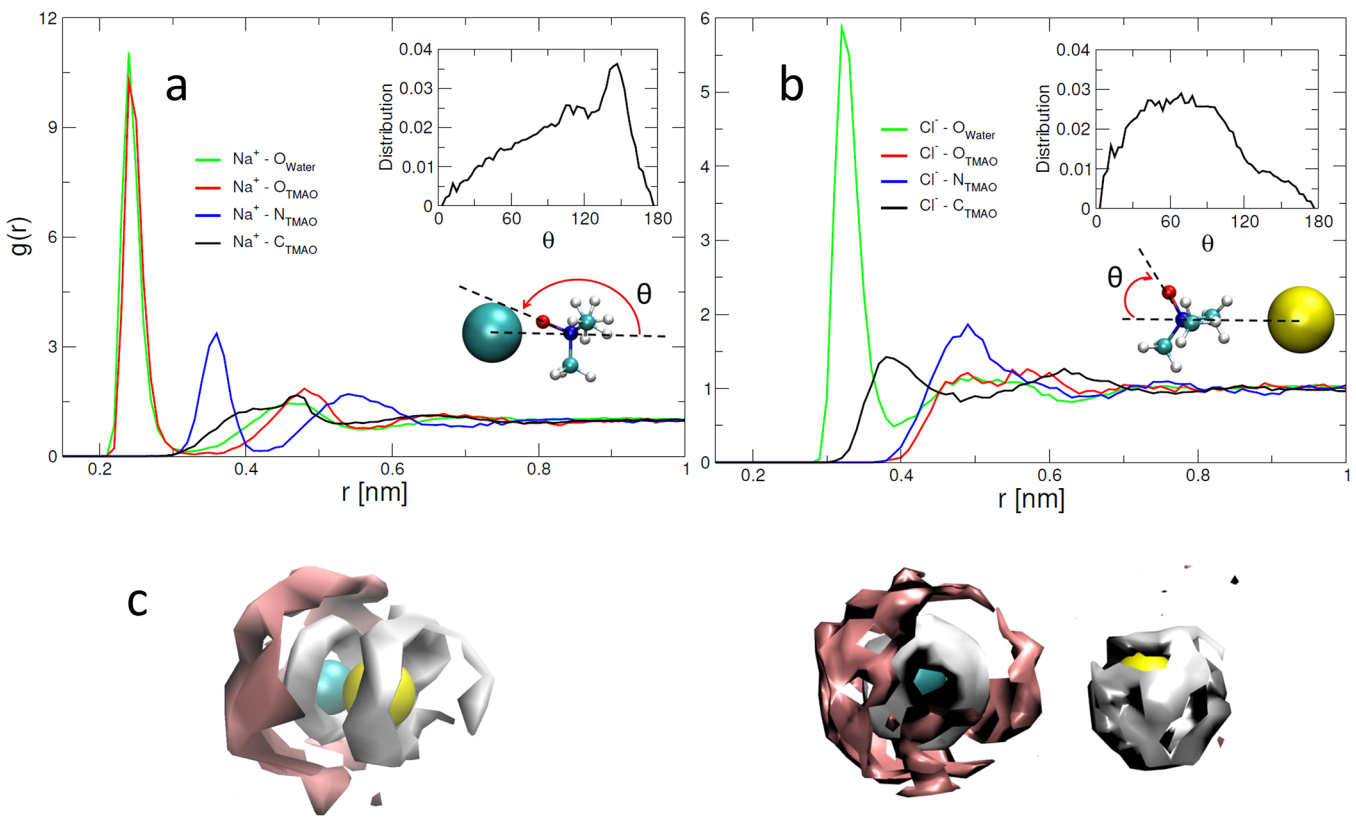

Figure 9. (a, b) RDFs of ions and different atoms of TMAO (oxygen in red, nitrogen in blue, and carbon in black) or water (green) for simulations performed in 7 M Kast TMAO solution when ions are far apart, i.e., ξ = 1.1 nm. Inset panels show the distribution of θ in the solvation shell. (c) Spatial distribution functions of TMAO (pink color) and water (silver color) around ions in 7 M Kast TMAO solution at ξ = 0.375 nm (left) and at ξ = 1.1 nm (right). Isovalues for TMAO and water are 7.5 and 10.

DOI: 10.1021/acs.jpcb.7b11847
J. Phys. Chem. B XXXX, XXX, XXX−XXX

suggests that methyl groups of TMAO are solvated away from this ion. Accordingly, the distribution of θ (defined in Figure 9a for TMAO molecules that are in the solvation shell) is biased toward large angles, see inset of Figure 9a. This characterizes TMAO orientations in which O_{TMAO} atoms point toward Na^+ and C_{TMAO} atoms point away from this ion.

Figure 9b shows that RDFs of Cl^- and different atoms of TMAO are not characterized by a strong first peak. Moreover, only a reduced number of C_{TMAO} atoms are located within the first solvation shell around the Cl^- ion. This suggests exclusion of TMAO's polar group from the vicinity of Cl^-. Accordingly, the distribution of θ in the inset of Figure 9b is biased toward short angles corresponding to oxygen atoms of TMAO pointing away from Cl^-.

In Figure 9c, we show spatial distributions of TMAO (in pink) and water (silver) around Na^+ and Cl^- when these ions are far apart (ξ = 1.1 nm) and at cm (ξ = 0.375 nm). In agreement with RDF in Figure 9a,b, these spatial distribution functions provide evidence that the solvation shell of Na^+ contains both water and TMAO molecules whereas the solvation shell around Cl^- contains mainly water molecules.

CONCLUSION

In this article, we studied effects of TMAO on hydrophobic interactions by considering two neopentane models (i.e., a five-site model and the all-atom AMBER model) and two TMAO models (i.e., Kast and Netz models). Computed PMFs show that Netz TMAO favors hydrophobic association of both models of neopentane whereas Kast TMAO has no significant effect on the all-atom AMBER model and it destabilizes the association of the five-site model. This shows that force-fields play an important role on how TMAO affects hydrophobic interactions in simulations. Results depend not only on TMAO's force-field but also on the model of nonpolar molecules used in the simulations. This calls for caution when extrapolating results from model compounds to proteins. Accordingly, PMFs from our all-atom simulations suggest that peptides made from mostly nonpolar side chains that resemble neopentane (e.g., valine and leucine) would adopt more compact conformations when TMAO is added to aqueous solution. However, in a recent study, TMAO was shown to have the opposite effect; i.e., it swells 10-residue homovaline and homoleucine peptides. The former study was performed using the AMBER99sb-ILDN-force-field which is compatible with the AMBER force-field used in this work for neopentane. Moreover, effects of TMAO on polyvaline and polyleucine peptides were demonstrated to be robust against details of TMAO's force-field.

In this work, we also quantified entropic and enthalpic contributions of hydrophobic interactions in pure water and aqueous TMAO solutions. Both the large favorable change in the entropy component and the unfavorable change in enthalpy that emerge upon the association of small nonpolar molecules in water become smaller when TMAO is added to the solution. The combined effects of these enthalpic and entropic changes account for a negligible effect and a stabilizing effect on the association of neopentane molecules when Kast and Netz models are used in the simulations, respectively. Effects of TMAO on the enthalpy are mainly due to changes in the potential energy involving solvent−solvent molecules. We show that the presence of TMAO in the solvation shell of neopentane may explain its effect on the enthalpy and the entropy components.

To provide insights into how TMAO affects charged interactions in aqueous solution, we study the association of Na^+ and Cl^- ions. Kast and Netz models are used to mimic TMAO. Both TMAO models are found to stabilize the interaction between Na^+ and Cl^- as they reduce the enthalpic penalty of bringing these ions together. The enthalpy is reduced because TMAO has a strong effect on ion−solvent interactions. We find that TMAO is attracted to Na^+ becoming part of its solvation shell whereas it is excluded from the vicinity of Cl^-.

ASSOCIATED CONTENT

Supporting Information

The Supporting Information is available free of charge on the ACS Publications website at DOI: 10.1021/acs.jpcb.7b11847.

Parameters of Kast and Netz force-fields, list and details of the different simulations performed in this work, PMFs of neopentane dimers and sodium chloride ions at different temperatures, RDFs of $C_{central}$ and different atoms of TMAO, heat capacity, analysis of first SSM for ions in 7 M Netz TMAO solution, and PMF of charge−charge interactions computed using Joung and Cheatham force-field (PDF)

AUTHOR INFORMATION

Corresponding Author

*E-mail: cld@njit.edu.

ORCID

Cristiano L. Dias: 0000-0002-8765-3922

Notes

The authors declare no competing financial interest.

ACKNOWLEDGMENTS

This work was funded by a grant from the ACS-PRF#58024-ND6 and by NJIT. Computational resources for this work were provided by Compute Canada.

REFERENCES

(1) Yancey, P. H. Organic osmolytes as compatible, metabolic and counteracting cytoprotectants in high osmolarity and other stresses. *J. Exp. Biol.* **2005**, *208*, 2819−2830.

(2) Yancey, P. H.; Clark, M. E.; Hand, S. C.; Bowlus, R. D.; Somero, G. N. Living with water stress: evolution of osmolyte systems. *Science* **1982**, *217*, 1214−1222.

(3) Yancey, P. Proteins and counteracting osmolytes. *Biologist* **2003**, *50*, 126−131.

(4) Schroer, M. A.; Zhai, Y.; Wieland, D.; Sahle, C. J.; Nase, J.; Paulus, M.; Tolan, M.; Winter, R. Exploring the piezophilic behavior of natural cosolvent mixtures. *Angew. Chem., Int. Ed.* **2011**, *50*, 11413−11416.

(5) Street, T. O.; Bolen, D. W.; Rose, G. D. A molecular mechanism for osmolyte-induced protein stability. *Proc. Natl. Acad. Sci. U. S. A.* **2006**, *103*, 13997−14002.

(6) Jas, G. S.; Rentchler, E. C.; Słowicka, A. M.; Hermansen, J. R.; Johnson, C. K.; Middaugh, C. R.; Kuczera, K. Reorientation motion and preferential interactions of a peptide in denaturants and osmolyte. *J. Phys. Chem. B* **2016**, *120*, 3089−3099.

(7) Holehouse, A. S.; Garai, K.; Lyle, N.; Vitalis, A.; Pappu, R. V. Quantitative assessments of the distinct contributions of polypeptide backbone amides versus side chain groups to chain expansion via chemical denaturation. *J. Am. Chem. Soc.* **2015**, *137*, 2984−2995.

(8) de Oliveira, G. A.; Silva, J. L. A hypothesis to reconcile the physical and chemical unfolding of proteins. *Proc. Natl. Acad. Sci. U. S. A.* **2015**, *112*, E2775−E2784.

DOI: 10.1021/acs.jpcb.7b11847
J. Phys. Chem. B XXXX, XXX, XXX−XXX

(9) Su, Z.; Dias, C. L. Molecular interactions accounting for protein denaturation by urea. *J. Mol. Liq.* **2017**, *228*, 168−175.
(10) Zangi, R.; Zhou, R.; Berne, B. Urea's action on hydrophobic interactions. *J. Am. Chem. Soc.* **2009**, *131*, 1535−1541.
(11) Linhananta, A.; Hadizadeh, S.; Plotkin, S. S. An effective solvent theory connecting the underlying mechanisms of osmolytes and denaturants for protein stability. *Biophys. J.* **2011**, *100*, 459−468.
(12) Arakawa, T.; Timasheff, S. The stabilization of proteins by osmolytes. *Biophys. J.* **1985**, *47*, 411−414.
(13) Gillett, M. B.; Suko, J. R.; Santoso, F. O.; Yancey, P. H. Elevated levels of trimethylamine oxide in muscles of deep-sea gadiform teleosts: A high-pressure adaptation. *J. Exp. Zool.* **1997**, *279*, 386−391.
(14) Yancey, P. H.; Gerringer, M. E.; Drazen, J. C.; Rowden, A. A.; Jamieson, A. Marine fish may be biochemically constrained from inhabiting the deepest ocean depths. *Proc. Natl. Acad. Sci. U. S. A.* **2014**, *111*, 4461−4465.
(15) Canchi, D. R.; García, A. E. Cosolvent effects on protein stability. *Annu. Rev. Phys. Chem.* **2013**, *64*, 273−293.
(16) Courtenay, E.; Capp, M.; Anderson, C.; Record, M. Vapor pressure osmometry studies of osmolyte-protein interactions: implications for the action of osmoprotectants in vivo and for the interpretation of osmotic stress experiments in vitro. *Biochemistry* **2000**, *39*, 4455−4471.
(17) Lin, T.-Y.; Timasheff, S. N. Why do some organisms use a urea-methylamine mixture as osmolyte? Thermodynamic compensation of urea and trimethylamine N-oxide interactions with protein. *Biochemistry* **1994**, *33*, 12695−12701.
(18) Smolin, N.; Voloshin, V. P.; Anikeenko, A. V.; Geiger, A.; Winter, R.; Medvedev, N. N. TMAO and urea in the hydration shell of the protein SNase. *Phys. Chem. Chem. Phys.* **2017**, *19*, 6345−6357.
(19) Hunger, J.; Tielrooij, K.-J.; Buchner, R.; Bonn, M.; Bakker, H. J. Complex formation in aqueous trimethylamine-N-oxide (TMAO) solutions. *J. Phys. Chem. B* **2012**, *116*, 4783−4795.
(20) Bennion, B. J.; Daggett, V. Counteraction of urea-induced protein denaturation by trimethylamine N-oxide: a chemical chaperone at atomic resolution. *Proc. Natl. Acad. Sci. U. S. A.* **2004**, *101*, 6433−6438.
(21) Zou, Q.; Bennion, B. J.; Daggett, V.; Murphy, K. P. The molecular mechanism of stabilization of proteins by TMAO and its ability to counteract the effects of urea. *J. Am. Chem. Soc.* **2002**, *124*, 1192−1202.
(22) Munroe, K. L.; Magers, D. H.; Hammer, N. I. Raman spectroscopic signatures of noncovalent interactions between trimethylamine N-oxide (TMAO) and water. *J. Phys. Chem. B* **2011**, *115*, 7699−7707.
(23) Sagle, L. B.; Cimatu, K.; Litosh, V. A.; Liu, Y.; Flores, S. C.; Chen, X.; Yu, B.; Cremer, P. S. Methyl groups of trimethylamine N-oxide orient away from hydrophobic interfaces. *J. Am. Chem. Soc.* **2011**, *133*, 18707−18712.
(24) Koga, Y.; Westh, P.; Nishikawa, K.; Subramanian, S. Is a methyl group always hydrophobic? Hydrophilicity of trimethylamine-N-oxide, tetramethyl urea and tetramethylammonium ion. *J. Phys. Chem. B* **2011**, *115*, 2995−3002.
(25) Schneck, E.; Horinek, D.; Netz, R. R. Insight into the Molecular Mechanisms of Protein Stabilizing Osmolytes from Global Force-Field Variations. *J. Phys. Chem. B* **2013**, *117*, 8310−8321.
(26) Bolen, D. W.; Rose, G. D. Structure and energetics of the hydrogen-bonded backbone in protein folding. *Annu. Rev. Biochem.* **2008**, *77*, 339−362.
(27) Auton, M.; Bolen, D. W.; Rösgen, J. Structural thermodynamics of protein preferential solvation: osmolyte solvation of proteins, aminoacids, and peptides. *Proteins: Struct., Funct., Genet.* **2008**, *73*, 802−813.
(28) Auton, M.; Ferreon, A. C. M.; Bolen, D. W. Metrics that differentiate the origins of osmolyte effects on protein stability: a test of the surface tension proposal. *J. Mol. Biol.* **2006**, *361*, 983−992.
(29) Auton, M.; Bolen, D. W. Chapter Twenty-Three-Application of the Transfer Model to Understand How Naturally Occurring Osmolytes Affect Protein Stability. *Methods Enzymol.* **2007**, *428*, 397−418.
(30) Hu, C. Y.; Lynch, G. C.; Kokubo, H.; Pettitt, B. M. Trimethylamine N-oxide influence on the backbone of proteins: An oligoglycine model. *Proteins: Struct., Funct., Genet.* **2010**, *78*, 695−704.
(31) Su, Z.; Mahmoudinobar, F.; Dias, C. L. Effects of Trimethylamine-N-oxide on the Conformation of Peptides and its Implications for Proteins. *Phys. Rev. Lett.* **2017**, *119*, 108102−6.
(32) Rodriguez-Ropero, F.; Rötzscher, P.; van der Vegt, N. F. Comparison of Different TMAO Force Fields and Their Impact on the Folding Equilibrium of a Hydrophobic Polymer. *J. Phys. Chem. B* **2016**, *120*, 8757−8767.
(33) Mondal, J.; Stirnemann, G.; Berne, B. When does trimethylamine N-oxide fold a polymer chain and urea unfold it? *J. Phys. Chem. B* **2013**, *117*, 8723−8732.
(34) Cho, S. S.; Reddy, G.; Straub, J. E.; Thirumalai, D. Entropic stabilization of proteins by TMAO. *J. Phys. Chem. B* **2011**, *115*, 13401−13407.
(35) Ma, J.; Pazos, I. M.; Gai, F. Microscopic insights into the protein-stabilizing effect of trimethylamine N-oxide (TMAO). *Proc. Natl. Acad. Sci. U. S. A.* **2014**, *111*, 8476−8481.
(36) Liao, Y.-T.; Manson, A. C.; DeLyser, M. R.; Noid, W. G.; Cremer, P. S. Trimethylamine N-oxide stabilizes proteins via a distinct mechanism compared with betaine and glycine. *Proc. Natl. Acad. Sci. U. S. A.* **2017**, *114*, 2479−2484.
(37) Fiore, A.; Venkateshwaran, V.; Garde, S. Trimethylamine N-oxide (TMAO) and tert-butyl alcohol (TBA) at hydrophobic interfaces: Insights from molecular dynamics simulations. *Langmuir* **2013**, *29*, 8017−8024.
(38) Athawale, M. V.; Dordick, J. S.; Garde, S. Osmolyte trimethylamine-N-oxide does not affect the strength of hydrophobic interactions: origin of osmolyte compatibility. *Biophys. J.* **2005**, *89*, 858−866.
(39) Sarma, R.; Paul, S. Association of small hydrophobic solute in presence of the osmolytes urea and trimethylamine-N-oxide. *J. Phys. Chem. B* **2012**, *116*, 2831−2841.
(40) Athawale, M. V.; Sarupria, S.; Garde, S. Enthalpy-entropy contributions to salt and osmolyte effects on molecular-scale hydrophobic hydration and interactions. *J. Phys. Chem. B* **2008**, *112*, 5661−5670.
(41) Ganguly, P.; van der Vegt, N. F.; Shea, J.-E. Hydrophobic association in mixed urea-TMAO solutions. *J. Phys. Chem. Lett.* **2016**, *7*, 3052−3059.
(42) Paul, S.; Patey, G. The influence of urea and trimethylamine-N-oxide on hydrophobic interactions. *J. Phys. Chem. B* **2007**, *111*, 7932−7933.
(43) Markthaler, D.; Zeman, J.; Baz, J.; Smiatek, J.; Hansen, N. Validation of Trimethylamine-N-oxide (TMAO) Force Fields Based on Thermophysical Properties of Aqueous TMAO Solutions. *J. Phys. Chem. B* **2017**, *121*, 10674−10688.
(44) Schneck, E.; Horinek, D.; Netz, R. R. Insight into the Molecular Mechanisms of Protein Stabilizing Osmolytes from Global Force-Field Variations. *J. Phys. Chem. B* **2013**, *117*, 8310−8321.
(45) Lee, M.-E.; van der Vegt, N. F. Does urea denature hydrophobic interactions? *J. Am. Chem. Soc.* **2006**, *128*, 4948−4949.
(46) Hess, B.; Kutzner, C.; van der Spoel, D.; Lindahl, E. GROMACS 4: Algorithms for Highly Efficient, Load-Balanced, and Scalable Molecular Simulation. *J. Chem. Theory Comput.* **2008**, *4*, 435−447.
(47) Kast, K. M.; Brickmann, J.; Kast, S. M.; Berry, R. S. Binary phases of aliphatic N-oxides and water: Force field development and molecular dynamics simulation. *J. Phys. Chem. A* **2003**, *107*, 5342−5351.
(48) Jorgensen, W. L.; Maxwell, D. S.; Tirado-Rives, J. Development and testing of the OPLS all-atom force field on conformational energetics and properties of organic liquids. *J. Am. Chem. Soc.* **1996**, *118*, 11225−11236.
(49) Sangster, M.; Atwood, R. Interionic potentials for alkali halides. II. Completely crystal independent specification of Born-Mayer potentials. *J. Phys. C: Solid State Phys.* **1978**, *11*, 1541.

DOI: 10.1021/acs.jpcb.7b11847
J. Phys. Chem. B XXXX, XXX, XXX−XXX

(50) Hölzl, C.; Kibies, P.; Imoto, S.; Frach, R.; Suladze, S.; Winter, R.; Marx, D.; Horinek, D.; Kast, S. M. Design principles for high-pressure force fields: Aqueous TMAO solutions from ambient to kilobar pressures. *J. Chem. Phys.* **2016**, *144*, 144104.
(51) Hub, J. S.; De Groot, B. L.; Van Der Spoel, D. g_wham A Free Weighted Histogram Analysis Implementation Including Robust Error and Autocorrelation Estimates. *J. Chem. Theory Comput.* **2010**, *6*, 3713−3720.
(52) Shimizu, S.; Chan, H. S. Temperature dependence of hydrophobic interactions: A mean force perspective, effects of water density, and nonadditivity of thermodynamic signatures. *J. Chem. Phys.* **2000**, *113*, 4683−4700.
(53) Kunugi, S.; Tanaka, N. Cold denaturation of proteins under high pressure. *Biochim. Biophys. Acta, Protein Struct. Mol. Enzymol.* **2002**, *1595*, 329−344.
(54) Dias, C. L.; Ala-Nissila, T.; Wong-ekkabut, J.; Vattulainen, I.; Grant, M.; Karttunen, M. The Hydrophobic Effect and its Role in Cold Denaturation. *Cryobiology* **2010**, *60*, 91−99.
(55) Pratt, L. R.; Chandler, D. Theory of the hydrophobic effect. *J. Chem. Phys.* **1977**, *67*, 3683−3704.
(56) Dias, C. L.; Hynninen, T.; Ala-Nissila, T.; Foster, A. S.; Karttunen, M. Hydrophobicity within the three-dimensional Mercedes-Benz model: Potential of mean force. *J. Chem. Phys.* **2011**, *134*, 065106.
(57) Southall, N. T.; Dill, K. A. Potential of mean force between two hydrophobic solutes in water. *Biophys. Chem.* **2002**, *101−102*, 295−307.
(58) Dias, C. L.; Chan, H. S. Pressure-Dependence Properties of Elementary Hydrophobic Interactions: Ramifications for Activation Properties of Protein Folding. *J. Phys. Chem. B* **2014**, *118*, 7488−7509.
(59) Dias, C. L. Unifying Microscopic Mechanism for Pressure and Cold Denaturations of Proteins. *Phys. Rev. Lett.* **2012**, *109*, 048104−048109.
(60) Frank, H. S.; Evans, M. W. Free volume and entropy in condensed systems III. Entropy in binary liquid mixtures; partial molal entropy in dilute solutions; structure and thermodynamics in aqueous electrolytes. *J. Chem. Phys.* **1945**, *13*, 507−532.
(61) Dill, K. A. Dominant forces in protein folding. *Biochemistry* **1990**, *29*, 7133−7155.
(62) Dias, C. L.; Ala-Nissila, T.; Karttunen, M.; Vattulainen, I.; Grant, M. Microscopic Mechanism for Cold Denaturation. *Phys. Rev. Lett.* **2008**, *100*, 118101−118105.
(63) Patra, M.; Karttunen, M. Systematic comparison of force fields for microscopic simulations of NaCl in aqueous solutions: diffusion, free energy of hydration, and structural properties. *J. Comput. Chem.* **2004**, *25*, 678−689.
(64) Timko, J.; Bucher, D.; Kuyucak, S. Dissociation of NaCl in water from ab initio molecular dynamics simulations. *J. Chem. Phys.* **2010**, *132*, 114510.
(65) Joung, I. S.; Cheatham, T. E., III Determination of alkali and halide monovalent ion parameters for use in explicitly solvated biomolecular simulations. *J. Phys. Chem. B* **2008**, *112*, 9020−9041.
(66) Yui, K.; Sakuma, M.; Funazukuri, T. Molecular dynamics simulation on ion-pair association of NaCl from ambient to supercritical water. *Fluid Phase Equilib.* **2010**, *297*, 227−235.
(67) Dill, K.; Bromberg, S. *Molecular Driving Forces: Statistical Thermodynamics in Biology, Chemistry, Physics, and Nanoscience*; Garland Science, 2010.

DOI: 10.1021/acs.jpcb.7b11847
J. Phys. Chem. B XXXX, XXX, XXX−XXX